applied sciences

MDPI

Article

Influence and Optimization of Geometric Parameters for Small-Radius Curved Tunnel Based on Response Surface Method

Xiaojiu Feng *, Yongtian Xie, Shaofeng Liu and Fujian Yang

School of Urban Construction, Changzhou University, Changzhou 213164, China
* Correspondence: fengxiaojiu@cczu.edu.cn

Abstract: Compared with straight tunnels, small-radius curved tunnels are more common and have more complex influencing factors in urban underground traffic. Therefore, the seismic evaluation of small-radius curved tunnels is of great significance for the safe operation of underground structures. This paper used numerical analysis and the response surface method to analyze the influence of buried depth, curve angle and curve radius on the seismic response of a small-radius curved tunnel. For this purpose, seventeen three-dimensional (3D) numerical analysis models of the small-radius curved tunnel considering different geometric parameters are established. In addition, the optimal geometric parameters of displacement response and acceleration response of the small-radius curved tunnel are studied by using the method of multi-objective optimization design. The results show that buried depth has a pronounced influence upon the displacement response of the small-radius curved tunnel, whilst the buried depth and curve radius are the key parameters affecting the acceleration response of the small-radius curved tunnel. The optimal parameter configuration of the small-radius curved tunnel is the maximum buried depth, the maximum curve angle and the maximum curve radius within the value domain.

Keywords: small-radius curved tunnel; response surface method; finite element simulation; multi-objective optimization

Citation: Feng, X.; Xie, Y.; Liu, S.; Yang, F. Influence and Optimization of Geometric Parameters for Small-Radius Curved Tunnel Based on Response Surface Method. *Appl. Sci.* **2023**, *13*, 3800. https://doi.org/10.3390/app13063800

Academic Editor: José António Correia

Received: 17 February 2023
Revised: 12 March 2023
Accepted: 14 March 2023
Published: 16 March 2023

1. Introduction

With the rapid development of large and medium-sized cities in the world and the increasing population, the traditional ground transportation system has been unable to meet people's traffic needs. Therefore, a lot of cities have built or are building a large number of underground railways. As a result of the limitations of early urban traffic planning, in the process of subway construction, the line planning needs to bypass some large buildings that have been built, resulting in a large number of curved tunnels. Compared with a straight section tunnel, the seismic response of a curved tunnel is more complex, especially for a small-radius curved tunnel; because of its small bending radius and irregular trend, the influence factors of its seismic performance are more complex. Therefore, it is necessary to conduct in-depth research on the seismic response of small-radius curve tunnels under different influence factors to ensure the stability of subway lines and surface buildings.

Finite element numerical simulation technology is extensively utilized for the seismic analysis of underground structures owing to its economy and easy operation. After many years of research, a large number of researchers have made great progress regarding the seismic performance to tunnels. Choi et al. [1] combined ANSYS finite element simulation (FEM) software with linear soil–structure interaction (SSI) codes for studying the non-linear seismic dynamic response of subterranean box constructions and determined the relevant factors affecting their seismic performance. Chen et al. [2] examined the seismic response of a tunnel model of an integrated pipe corridor driven by uneven seismic stimulation by means of numerical simulation for comparison with experimental results.

It was found that the integrated pipe corridor underwent bending deformation, and the acceleration response was greater than the surrounding soil, and the modelling approach in this study was reasonable for shaking table tests. Ding et al. [3] proposed a numerical simulation method pertaining to massive seismic response calculations in sunken tube tunnels. The finite element LS-DYNA analysis software was applied to add flexible joints to the weak parts of the tunnel under seismic excitation, which effectively controlled the displacement of the tunnel section. Kontoe et al. [4] investigated the seismic response of a double tunnel using statically and dynamically plane strain finite element analysis, respectively, and compared the results with seismic field observations. It was found that the tunnel deformation was predominantly elliptical and that the interaction of the tunnel pillars with the wave reflection between the columns had little effect on its seismic performance. In addition, many academicians have carried out research on the seismic response, seismic design and calculation methods for subterranean constructions such as tunnels. Shukla et al. [5] investigated the seismic load effects on tunnels and shafts under seismic excitation by proposing a closed form idea, which is applicable to tunnels and shafts of small length. Anastasopoulos et al. [6] examined the non-linear response of deep sunken tunnels subject to strong earthquakes. Sánchez-Merino et al. [7] investigated the lengthwise seismic response of tunnel interlined structures under frontal waves. Dowding and Rozan [8] studied the damage of rock tunnels under ground shaking.

However, most of the above researchers have based their studies on straight-line tunnels. Research into the seismic response of curved tunnels has been in its infancy in recent years, and researchers have only proposed relevant research ideas, without forming a complete research system. Mu and Wang [9] explored the effect of small-radius curved tunnels under unidirectional horizontal seismic excitation regarding curve angle, vibration amplitude and other factors on tunnel seismic response using FEM analysis, which found that a curved tunnel section has less effect on tunnel acceleration and more effect on tunnel deformation, but the effects of specific relevant geometric parameters such as buried depth and curve radius with respect to seismic response of small-radius curved tunnels was not addressed in the paper.

The paper aims to discuss the implications of designing and optimizing multiple geometric parameters configuration on the seismic response of small-radius curved tunnels. The 3D numerical analysis model of geometrical parameters such as buried depth, curve angle and curve radius of small-radius curved tunnels are designed and established to investigate the interactive effects on displacement response and acceleration response under seismic excitation by utilizing finite element analysis software ABAQUS 2022 and response surface methodology (RSM) software Design-Expert V12. In addition, a multi-objective optimization design (MOOD) approach is used to achieve the minimum displacement and acceleration objectives.

2. Methodology

2.1. 3D Finite Element Model

As a typical underground structure, tunnels are widely used as underground transportation in major cities in the world. Therefore, the seismic safety of tunnel structure is very important. It is found that the complex soil–structure interaction (SSI) effect linking the tunnel to the surrounding soil exerts uncertain consequences upon the seismic behavior of the tunnel structure. To this end, in order to consider the SSI effect between small-radius curved tunnel and the surrounding soil, the widely used viscous-spring artificial boundary (VSAB) for simulating the elastic recovery behavior of infinite foundations is adopted. In the VSAB method, the seismic acceleration acts on the artificial boundary node in the form of equivalent load through calculation [10]. The applicability and accuracy of VSAB and seismic input method have been verified in many literatures [11–14]. Therefore, 3D finite element models are established based on the above literature.

The Mohr–Coulomb constitutive model [15] is adopted for the soil. The 3D numerical finite element models are shown in Figure 1.

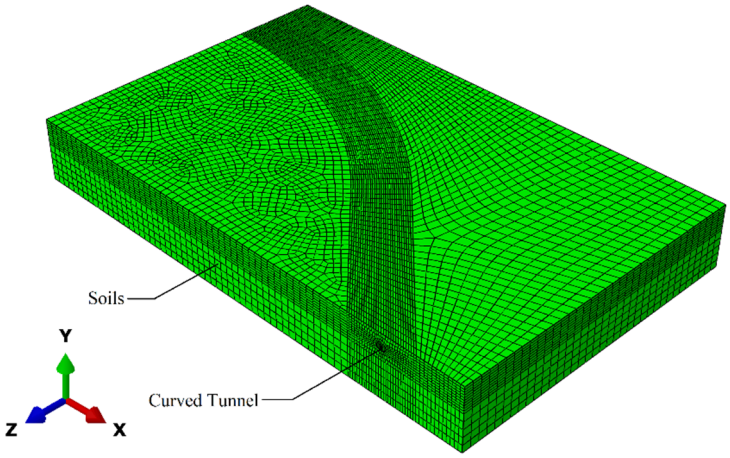

Figure 1. Three-dimensional numerical models of small-radius curved tunnel and surrounding soil.

2.2. Response Surface Methodology

In recent years, owing to the research and development of statistics in various fields, with the deepening of numerical science calculation, more and more domestic and foreign researchers in aviation, aerospace, vehicles, ships, machinery, chemical, food and materials science in the face of multi-objective optimization design (MOOD) are using response surface method (RSM). RSM has developed from the combination between mathematics and statistics to model and analyze the expected response value affected by multiple parameters. Its ultimate purpose is to optimize the response value by taking reasonable values of each parameter, to obtain the optimal designed results with minimum input [16].

The RSM was originally proposed in 1951 by Box and Wilson [17]. Chemical industry is the initial application area of RSM. Box and Draper [18] defined this method as a set of statistical approaches applied in the construction and development of empirical models. Hill and Hunter [19] introduced the research and application progress of RSM in chemical processes, demonstrating the regular analysis and multi-objective optimization problems with examples. Mead and Pike [20] made a summary of RSM and introduced the progress of RSM in biological research by enumerating the methods of work in related research fields. Myers et al. [16] brilliantly summarized the development and application of RSM theory from 1966 to 1988. Myers and Montgomery [21] comprehensively elaborated on the response surface method and its application and defined the method as a statistical and mathematical method for development, improvement and optimization. The test design includes the following two points [16].

(1) A result of unknown performance (called sample value) is obtained by testing in a certain sampling point (A point in a high-dimensional field, a set of design variables $x = (x_1, \cdots, x_n)^T$ as a sample point). Recently, the test has been extended from the physical test of the original instrument or equipment to the numerical analysis of the computer.
(2) To derive the function for unknown operational response, a sample value is far from enough. To acquire plural sampling points, it involves experimental design method of emission problem of a collection of sampling points in a high-dimensional field.

The construction of an approximation function of unknown performance from the sample values of a set of sample points is naturally called function fitting and known as regression statistics. The latter is the term in statistics, which means that the statistical treatment according to the results of the test, regression to the function to be sought, is also a very reasonable statement. In function fitting or regression statistics, the response surface method refers to an approach that constructs approximate models applied to industrial production design fields where it is rare or difficult to formulate the functionality between objectives, constraints and design variables with rigorous mathematical formulas.

2.3. RSM Model

To connect the seismic response of small-radius curved tunnel with the geometric parameters of the structure, response surface method (RSM) should be combined with numerical simulation. Firstly, the RSM model should be constructed. The RSM model can not only provide initial prediction for seismic response of small-radius curved tunnel, but also obtain which parameters have the greatest contribution to seismic response of tunnel structure. As shown in Figure 2, after verifying the accuracy of RSM model, RSM model is applied to structural optimization.

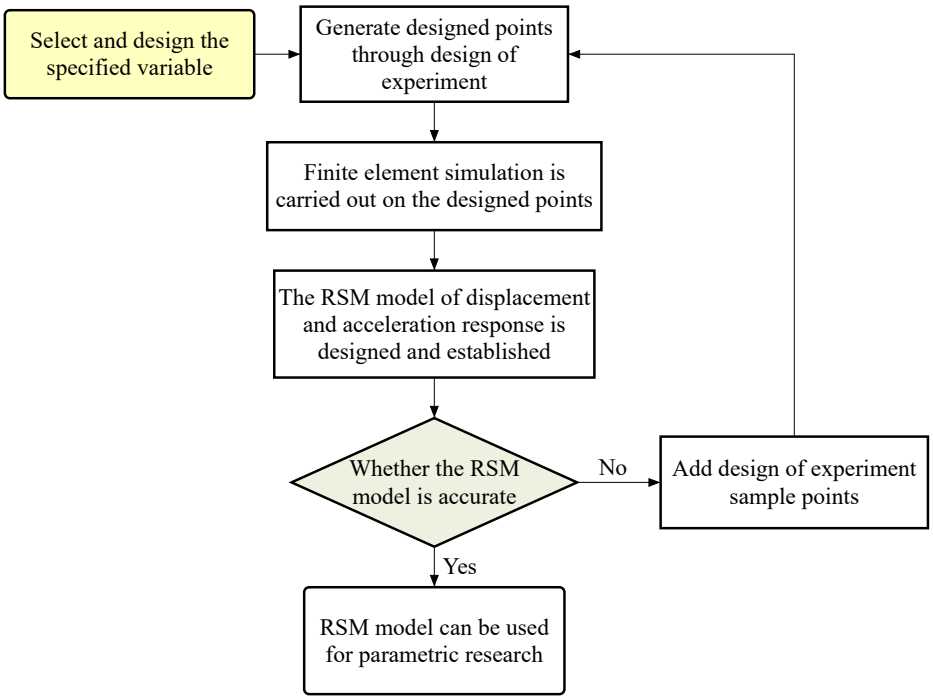

Figure 2. Modeling process of RSM model.

2.3.1. Sample Point Design

In the seismic response optimization design of small-radius curved tunnel, the deformation of the tunnel structure due to seismic excitation should be reduced; therefore, the displacement parameter of small-radius curved tunnel was selected as the first objective to minimize. At the same time, the vibration energy generated by the seismic excitation should not be excessive, so that the acceleration parameter of small-radius curved tunnel was selected as the second objective to minimize. In the parametric design, three main designed parameters are used, buried depth for small-radius curved tunnel, angle degree for curved tunnels and the curve radius R, so that they vary within a defined range. The seismic response of the tunnel structure is, therefore, formulated as follows:

$$\begin{cases} Max : (depth, \deg, R) \\ Min : (depth, \deg, R) \\ S.t\ x^l \le (depth, \deg, R) \le x^u \\ x = (depth, \deg, R) \end{cases} \quad (1)$$

where, $x = (x_1, x_2, \cdots, x_k)$ is a vector of k design variables of structural geometry $x^l = (x_1^l, x_2^l, \cdots, x_k^l)$ and $x^u = (x_1^u, x_2^u, \cdots, x_k^u)$ are the respective lower and upper bounds of the design variables. Due to high computational cost of quasi-static compression finite element simulation, it cannot be directly used to address the MOOD issues that requires several hundred performance evaluations. RSM model is widely used as an alternative model instead of non-linear finite element simulations to solve MOOD problems that

require fast iterations. In this paper, Design-Expert V12 statistical software is used for sample point design. A range of designed parameter values is selected through several FEM tests. The buried depth for the small-radius curved tunnel is 10–20 m, the angle deg of the curved tunnel is 45–60°and the curve radius R is 300–350 m, as shown in Table 1.

Table 1. Parameter setting and test design level.

Variable	Coded		
	−1	**0**	**1**
Depth of the curved tunnel, U (m)	10	15	20
Angle of the curved tunnel, V (deg)	45	52.5	60
Radius of curve, W (m)	300	325	350

The experimental design used a triple Box–Behnken response surface design type without embedding factors or partial factor designs. Through the experimental design, 17 sets of finite element simulations corresponding to different combinations of geometric parameters were conducted to derive the response values of each geometry combination to the displacement and acceleration of key points. The key point is to select the entrance endpoint A (Figure 3, Point A) of the small-radius curve tunnel and the connection point B (Figure 3, Point B) of the small-radius curve tunnel and the straight tunnel. The different combinations of design geometries and the corresponding response values are shown in Tables 2 and 3. Geometrical combinations for 17 different sets of parameters and the corresponding displacement (s) and acceleration (a) response values drawn from the FEM were input into Box–Behnken model of the statistical software Design-Expert V12 using the RSM. The polynomial equations (RSM model) were fitted to the FEM results using stepwise regression and identifying the relevant model terms. In this way, the constructed model and the individual terms in the regression equation can be checked for best fit results.

Table 2. The design matrix of Point A.

No.	Depth (m)	Angle (deg)	*R* (m)	*s* (m)	*a* (m/s^2)
1	10	45	325	0.12400	3.024
2	15	60	350	0.12000	3.602
3	20	60	325	0.11404	4.247
4	15	52.5	325	0.12005	4.152
5	10	52.5	300	0.12416	2.743
6	10	52.5	350	0.12411	2.931
7	15	52.5	325	0.12005	4.152
8	20	52.5	350	0.11404	2.185
9	15	52.5	325	0.12005	4.152
10	15	45	300	0.12008	4.659
11	15	52.5	325	0.12005	4.152
12	20	52.5	300	0.11403	4.410
13	15	45	350	0.12003	3.168
14	10	60	325	0.12407	3.096
15	20	45	325	0.11400	4.484
16	15	60	300	0.12000	3.358
17	15	52.5	325	0.12005	4.152

Table 3. The design matrix of Point B.

No.	Depth (m)	Angle (deg)	*R* (m)	*s* (m)	*a* (m/s^2)
1	10	45	325	0.12331	6.714
2	15	60	350	0.11923	6.122
3	20	60	325	0.11308	5.358
4	15	52.5	325	0.11911	7.442
5	10	52.5	300	0.12346	4.749
6	10	52.5	350	0.12345	4.791
7	15	52.5	325	0.11911	7.442
8	20	52.5	350	0.11297	11.985
9	15	52.5	325	0.11911	7.442
10	15	45	300	0.11907	8.979
11	15	52.5	325	0.11911	7.442
12	20	52.5	300	0.11286	13.738
13	15	45	350	0.11901	6.708
14	10	60	325	0.12362	3.756
15	20	45	325	0.11269	14.608
16	15	60	300	0.11917	5.492
17	15	52.5	325	0.11911	7.442

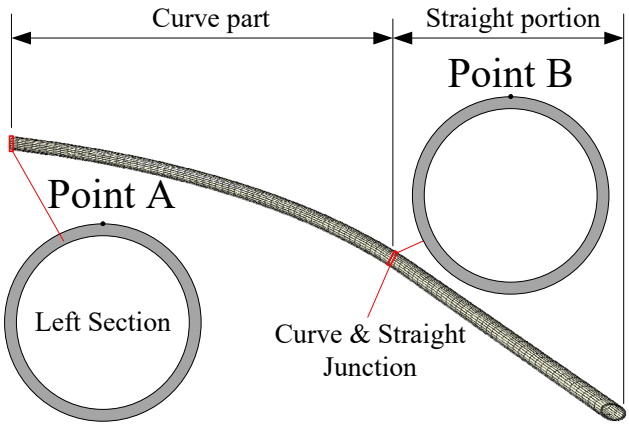

Figure 3. Layout of monitoring point of small-radius curve tunnel.

2.3.2. Numerical Analysis of RSM Model

The response values were analyzed by Design-Expert V12 software and the best fitting summary indicated that for the displacement (s) and acceleration (a) response of entrance point A of small-radius curved tunnel, the application of a quadratic model was recommended, and the adequacy of the developed model was tested using analysis of variance (ANOVA) methods. Tables 4 and 5 summarize the ANOVA of the responses and show the significance and adequacy measures of the models. The adequacy measures include the F-value and *p*-value of the model, the coefficient of determination R^2, the adjusted coefficient R^2, the prediction coefficient R^2 and the signal-to-noise ratio. Among them, F-value is used to evaluate the differences between groups and indicates the significance of the fitting equation of the RSM model. *p*-value is an indicator to measure the difference between the control group and the experimental group [21].

Table 4. Quadratic model ANOVA for displacement at point A.

Source	Sum of Squares	Mean Square	F-Value	*p*-Value	Significance [1]
Model	0.0002	0.0000	1.7995×10^4	<0.0001	***
U-Depth	0.0002	0.0002	1.5870×10^5	<0.0001	***
V-Angle	8.000×10^{-12}	8.000×10^{-12}	0.0063	0.9391	
W-R	9.901×10^{-10}	9.901×10^{-10}	0.7763	0.4075	
UV	2.560×10^{-10}	2.560×10^{-10}	0.2007	0.6677	
UW	8.123×10^{-10}	8.123×10^{-10}	0.6368	0.4511	
VW	1.024×10^{-9}	1.024×10^{-9}	0.8028	0.4000	
U^2	4.105×10^{-6}	4.105×10^{-6}	0.3218×10^4	<0.0001	***
V^2	7.121×10^{-9}	7.121×10^{-9}	5.58	0.0501	
W^2	1.164×10^{-9}	1.164×10^{-9}	0.9124	0.3713	
Residual	8.928×10^{-9}	1.275×10^{-9}			
Cor. total	0.0002				
R^2	1.0000	Coded Equation			
Adjusted R^2	0.9999	$\text{Sqrt}(s) = 0.12901 - 0.005U + 1 \times 10^{-6} \times V$			
Predicted R^2	0.9993	$-8 \times 10^{-6} \times UV - 0.001U^2$			
Adeq. Precision	370.57				

[1] Markers of significance factors: *** means highly significant.

Table 5. Quadratic model ANOVA for acceleration at point A.

Source	Sum of Squares	Mean Square	F-Value	*p*-Value	Significance [1]
Model	7.8900	0.8770	12.3600	0.0016	***
U-Depth	1.5600	1.5600	21.9800	0.0022	**
V-Angle	0.1331	0.1331	1.8800	0.2131	
W-R	1.3500	1.3500	19.0000	0.0033	*
UV	0.0239	0.0239	0.3365	0.5801	
UW	1.4600	1.4600	20.5200	0.0027	*
VW	0.7526	0.7526	10.6100	0.0139	
U^2	1.2000	1.2000	16.9500	0.0045	*
V^2	0.0381	0.0381	0.5370	0.4875	
W^2	1.2800	1.2800	12.3600	0.0038	*
Residual	0.4966	0.0709			
Cor. total	8.3900	Coded Equation			
R^2	0.9408	$\text{Sqrt}(a) = 4.15 + 0.4415U - 0.129V - 0.4105W$			
Adjusted R^2	0.8647	$-0.0733UV - 0.6033UW + 0.4337VW - 0.5344U^2$			
Predicted R^2	0.7908	$+0.0951V^2 - 0.5504W^2$			
Adeq. Precision	10.9503				

[1] Markers of significance factors: * means slightly significant; ** means moderate significant; *** means highly significant.

Table 4 shows the ANOVA results arising from the simplified linear model of the displacement response at point A. The F-value of the model is 1.7995×10^4, suggesting a significant model. The *p*-value of the model is less than 0.0001, indicating the extremely low likelihood of an F-value attributed to noise in this model. The prediction coefficient R^2 of 0.9993 corresponds well with the adjustment coefficient R^2 of 0.9999. The difference between the prediction coefficient R^2 and the adjustment coefficient R^2 is within 0.2, which is consistent with the results drawn from the extensive statistical documentation and fits with the corresponding literary results.

Furthermore, the signal-to-noise ratio of 370.57 is greater than the 4 specified in the relevant statistical literature, indicating that there is sufficient signal in the model and that the model has sufficient accuracy, and that there is no need to remove the relatively insignificant term to simplify the solution of the equation. The F-values of the designed

parameter variables shown in the model are available to denote the sequence of factors influencing the displacement response, and an ANOVA on Table 4 shows the buried depth of small-radius curved tunnel to be the greatest factor affecting displacement, with an F-value of 1.5870×10^5. The angle of the curved tunnel and the radius of the curve do not offer significant implications for the displacement response.

Table 5 presents the ANOVA results derived from the quadratic model of the acceleration response at point A. The model exhibits an F-value of 12.36 and a *p*-value of 0.0016, indicating the F-value of the model has a 0.16% probability of being caused by noise, so the model is significant. The prediction coefficient R^2 of 0.7908 is well-aligned with the adjustment coefficient R^2 of 0.8657, with a difference between the two coefficients within 0.2, in agreement with the relevant statistical literature. The signal-to-noise ratio of 10.9503 exceeds the value of 4 specified in the literature, confirming that the model features low noise and is suitable for parametric studies.

ANOVA on Table 5 reveals that the buried depth of the small-radius curved tunnel is the primary factor influencing acceleration, as evidenced by its high F-value of 21.98. The radius of the curved tunnel is also a significant factor affecting acceleration, while the angle of the curved tunnel does not significantly impact the acceleration response.

The response values were analyzed by Design-Expert software and the best fit output indicated that for the displacement and acceleration response of point B of small-radius curve tunnel, the application of quadratic and linear models was recommended and the adequacy of the developed models was tested using ANOVA methods. Tables 6 and 7 summarize the ANOVA of the responses and show the significance and adequacy measures of the models.

Table 6 shows the ANOVA results derived from the simplified quadratic model of the displacement response at point B. The model exhibits an F-value of 8782.04, suggesting a significant model. The *p*-value of the model is less than 0.0001, indicating an extremely low likelihood of an F-value attributed to noise in this model. The prediction coefficient R^2 of 0.9986 corresponds well with the adjustment coefficient R^2 of 0.9998, with a difference between the two coefficients within 0.2. The signal-to-noise ratio of 263.2664 surpasses the 4 specified in the relevant statistical literature, indicating that the model features adequate accuracy and signal strength. There is no need to simplify the solution of the equation by removing the relatively insignificant term.

Table 6. Quadratic model ANOVA for displacement at point B.

Source	Sum of Squares	Mean Square	F-Value	*p*-Value	Significance [1]
Model	0.0002	0.0000	8782.04	<0.0001	***
U-Depth	0.0002	0.0002	77,705.23	<0.0001	***
V-Angle	1.326×10^{-7}	1.326×10^{-7}	46.18	0.0003	**
W-R	9.901×10^{-10}	9.901×10^{-10}	0.3448	0.5755	
UV	2.116×10^{-9}	2.116×10^{-9}	0.7369	0.4191	
UW	2.756×10^{-9}	2.756×10^{-9}	0.9599	0.3599	
VW	3.600×10^{-9}	3.600×10^{-9}	1.25	0.2998	
U^2	3.668×10^{-6}	3.668×10^{-6}	1277.49	<0.0001	***
V^2	6.579×10^{-14}	6.579×10^{-14}	0.0000	0.9963	
W^2	3.901×10^{-10}	3.901×10^{-10}	0.1358	0.7233	
Residual	2.010×10^{-8}	2.871×10^{-8}			
Cor. total	0.0002				
R^2	0.9999	Coded Equation			
Adjusted R^2	0.9998	$\mathrm{Sqrt}(s) = 0.1191 - 0.0053U + 0.0001V$			
Predicted R^2	0.9986	$-0.0009U^2 - 1.25 \times 10^{-7}V^2 + 9.625 \times 10^{-6}W^2$			
Adeq. Precision	263				

[1] Markers of significance factors: ** means moderate significant; *** means highly significant.

Table 7. Quadratic model ANOVA for acceleration at point B.

Source	Sum of Squares	Mean Square	F-Value	*p*-Value	Significance [1]
Model	116.96	38.99	14.46	0.0002	***
U-Depth	82.42	82.42	30.57	<0.0001	***
V-Angle	33.13	33.13	12.29	0.0039	*
W-R	1.40	1.40	0.5210	0.4832	
Residual	35.05	2.70			
Cor. total	152.01				
R^2	0.7694	Coded Equation			
Adjusted R^2	0.7162	$\mathrm{Sqrt}(s) = 7.66 + 3.21U - 2.04V - 0.4190W$			
Predicted R^2	0.5189				
Adeq. Precision	13.1706				

[1] Markers of significance factors: * means slightly significant; *** means highly significant.

A comparison between the displacement response at point B (Table 6) and that at point A (Table 4) reveals that the angular F-value at point B is 46.18 with a *p*-value of 0.0003, while the angular F-value at point A is 0.0063 and has a *p*-value of 0.9391. These findings indicate that the angular factor at point B exerts a more significant impact on the displacement response than the angular factor at point A. Furthermore, the change in the angular factor at point B is more reliable for the results of the multi-objective optimized design.

The ANOVA analysis conducted on Table 6 reveals that the buried depth of the small-radius curved tunnel at point B is the primary influencing factor on displacement, as evidenced by the F-value of 77,705.23. Conversely, the radius of the curved tunnel does not demonstrate any statistically significant implications for displacement response. However, the angle of the small-radius curved tunnel exhibits a notable impact on the displacement response.

Table 7 presents the ANOVA results obtained from the linear model analysis of the acceleration response at point B. The computed F-value of 14.46 and *p*-value of 0.0002 indicate that there is a 0.02% probability that the F-value of the model is due to noise. Therefore, the model is deemed significant. The prediction coefficient R^2, which measures the proportion of the variance in the response variable explained by the independent variables, was found to be 0.51898, which corresponds well with the adjustment coefficient R^2 of 0.7162. The observed difference between the prediction and adjustment coefficients was within 0.2 and is consistent with the outcomes documented in extensive statistical literature and related studies.

Moreover, the signal-to-noise ratio of 13.1706 was calculated, which is greater than the threshold value of 4 recommended in the relevant statistical literature. This finding indicates that the model has very low noise and can be employed for parametric studies. Furthermore, the ANOVA reveals that the buried depth of the small-radius curved tunnel is the most significant factor affecting acceleration, with an F-value of 30.57, which is consistent with the ANOVA results for the acceleration response at point A. The angle of the small-radius curved tunnel has an F-value of 12.29 and a *p*-value of 0.0039, with a slightly significant implication for the acceleration response, while the radius of small-radius curved tunnel does not offer significant implications for the acceleration response.

2.3.3. Validation of the RSM Model

To demonstrate the validity of the RSM model, the seismic response results between FEM and the RSM predicted were compared; as shown in Table 8, the RSM predicted values were taken from the prediction options for selected factors in the Design-Expert software, and the developed RSM model was used to predict the displacement response and acceleration response, yielding a predicted displacement response of 0.114 m and an acceleration response of 3.487 m/s^2. The response values from the FEM were recalculated to correspond to the geometric parameters of 0.116 m displacement and 3.532 m/s^2 acceleration. Data

comparison shows that the error rates of 1.75% for displacement and 1.29% for acceleration are within acceptable tolerances, verifying the validity of the RSM model. The validity of the RSM model has been verified by point A, so the verification of the RS model at point B will not be repeated.

Table 8. Comparison between FEM results and RSM prediction results of point A.

Depth (m)	Angle (deg)	*R* (m)		*s* (m)	*a* (m/s^2)
20	60	338.24	FEM Results	0.116	3.532
			RSM Prediction	0.114	3.487
			Error	1.75%	1.29%

3. Analysis of the Response Surface Parameters

Based on the results of the experimental design, the influence of geometric parameters on the displacement response and acceleration response of the small-radius curved tunnel (point A and B) is further studied through parameter analysis.

3.1. Effects of Geometric Factors on the Displacement Response

The ANOVA in Table 4 of Section 2.3.2 has shown the buried depth of the small-radius curved tunnel to be the greatest factor affecting displacement. The angle of the curved tunnel and the radius of the curve do not offer significant implications for the displacement response. Figure 4 gives the variation of the displacement response of the small-radius curved tunnel under seismic excitation with respect to the buried depth and the angle of the curve. As can be seen from the figure, the displacement response of the small-radius curved tunnel under seismic excitation decreases as the buried depth increases, while the displacement response of the curved tunnel increases slightly as the angle increases. From Figure 4, it can be seen the minimum displacement response of the small-radius curved tunnel under seismic excitation is the maximum buried depth and minimum curve angle for the parameter design.

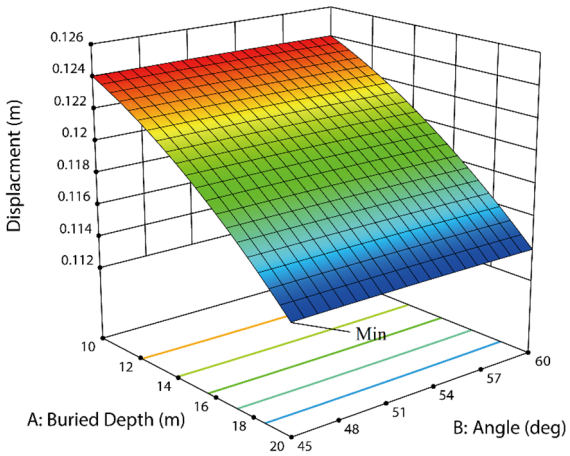

Figure 4. Variation of the displacement response with buried depth and angle at point A.

Based on the results of the experimental design, the influence of geometric parameters on the displacement response and acceleration response of the small-radius curved tunnel at point B is further studied through parameter analysis. The ANOVA in Table 6 already shows the buried depth of the small-radius curved tunnel to be the greatest factor affecting the displacement at point B. The angle of the curved tunnel is more consequential on the displacement response and the radius of the curve does not offer significant implications for the displacement response. In Figure 5, it can be seen the variation of the displacement response at point B under seismic excitation in the small-radius curved tunnel with respect

to the buried depth and the angle of the curve. From Figure 5, it can be seen that the displacement response of the small-radius curved tunnel under seismic excitation decreases as the buried depth increases, while the displacement response of the curved tunnel increases slightly as the angle increases. From Figure 5, it also can be seen that the minimum displacement response of the small-radius curved tunnel under seismic excitation is the parameter design for the maximum buried depth and the minimum curve angle. This conclusion is consistent with the analytical results for point A.

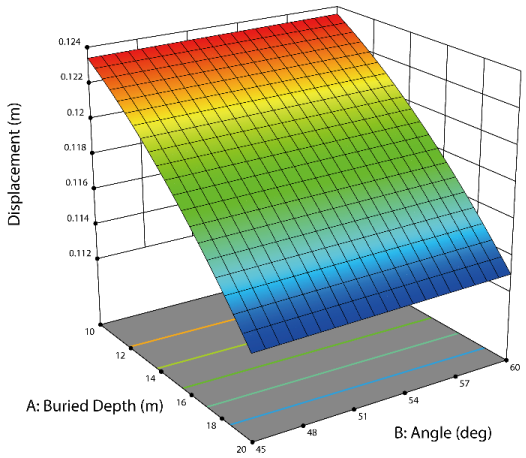

Figure 5. Variation of the displacement response with buried depth and radius at point B.

3.2. Effects of Geometric Factors on the Acceleration Response

The effects of two interactive factors on the acceleration response of point A are displayed in Figure 6. Figure 6a is for interactive buried depth and curve angle, while Figure 6b is for interactive buried depth and curve radius. From Figure 6a, it can be seen that the acceleration response of the small-radius curved tunnel under seismic excitation tends to increase and then decrease as the buried depth increases, with the minimum value of the acceleration response occurring around the minimum point of the buried depth, and the maximum point of the buried depth has a similarly small acceleration response. When the curve angle is 60°, the overall acceleration response is less than the curve angle of 45°. Figure 6b shows that when the curve radius reaches 300 m and the buried depth reaches 10 m, the acceleration response can be obtained at the minimum value; when the curve radius reaches 350 m and the buried depth reaches 20 m, the acceleration response value is also relatively small. When the curve radius reaches 350 m and the buried depth reaches 20 m, the acceleration response is also relatively small. Combined with Table 5, we can obtain that the buried depth and curve radius are the key parameters affecting the acceleration response value, and the effect of curve angle on the acceleration response value is not significant.

Figure 7 shows the significant effect of the interactive buried depth and curve radius on the acceleration response. The variation of acceleration response of point A with buried depth and curve radius for the small-radius curved tunnel under seismic excitation is given here, showing that the minimum acceleration can be obtained when both buried depth and curve radius are taken as minimum values.

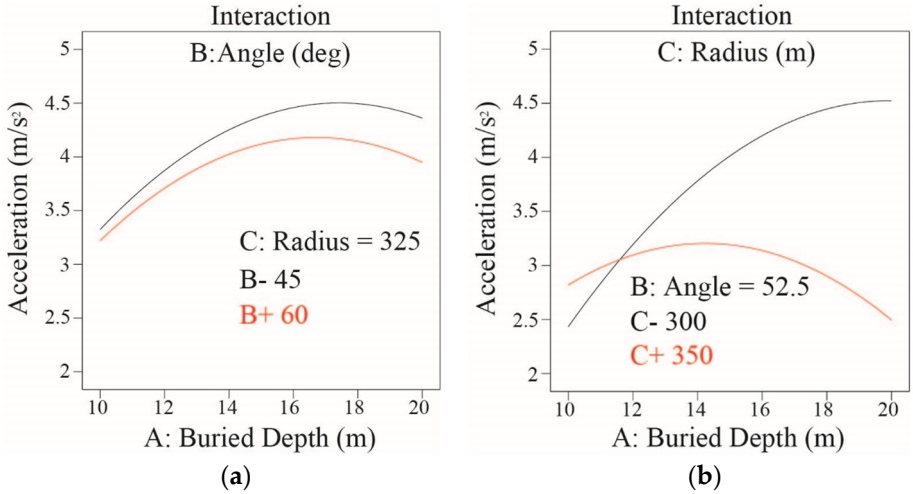

Figure 6. Interaction effect of buried depth on acceleration: (**a**) angle (deg); (**b**) radius (m).

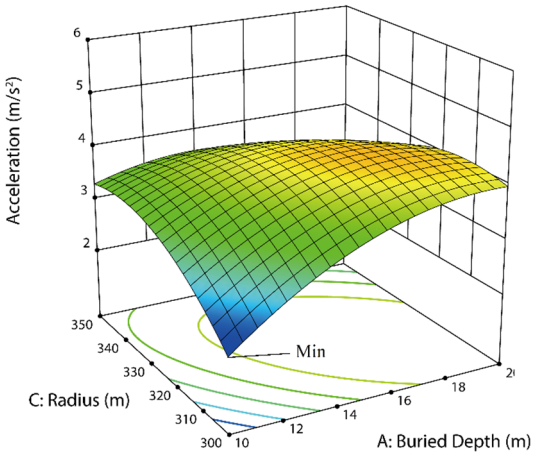

Figure 7. Variation of the acceleration response with buried depth and radius at point A.

Figure 8 shows the variation of the acceleration response at point B with buried depth and angle for the small-radius curved tunnel under seismic excitation, indicating that the smallest acceleration at point B can be obtained when the buried depth is taken as a minimum and the curve angle is taken as a maximum.

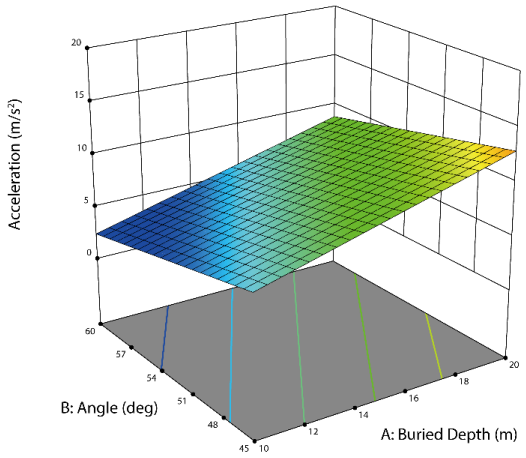

Figure 8. Variation of the acceleration response with buried depth and angle at point B.

4. Multi-Objective Optimization Design

Although the effects of miscellaneous parameters on the displacement response and acceleration response of the small-radius curved tunnel under seismic excitation are discussed above in the subsections, the specifics of how to optimize their design under seismic excitation are still unknown. In general, as part of the seismic response analysis, an optimum design is required for the various responses under study. A single-objective optimization approach that merely considers one objective has been employed in many previous investigations, and this approach is not applicable to almost all specific embodiments where multiple objectives need to be considered simultaneously. Therefore, it is more relevant to apply a MOOD approach to solve the optimal design for the seismic response of a small-radius curved tunnel.

4.1. Specification of the MOOD Problem

In line with the layout ideas discussed in Section 2.3.1 regarding sample point design, the displacement was selected as the first objective to minimize it. Simultaneously, the tunnel structure should not absorb excessive vibration energy, so the acceleration was selected as another objective to minimize it.

4.2. Design Method for MOOD Problem

MOOD problems can generally be solved by two methods: (1) solve all objectives separately and seek an optimum set of solutions; (2) transform the problem into a single-objective function by analyzing the importance of the different objective functions to obtain the corresponding weights and then multiplying them by the corresponding weights of the respective objectives, e.g., by using geometric averaging to obtain a single solution to the optimization design problem [22–25]. The second method can be used in Design-Expert software for optimal design and is characterized by low computational effort, fast convergence, flexible weighting and the possibility of assigning different weights to different objective responses.

4.3. Design Results of MOOD Problem

Building upon the RSM model established in Section 2.3.1, the MOOD takes the minimum displacement response and the minimum acceleration response as its objectives and formulates the modal problem of the small-radius curved tunnel under the action of seismic excitation as:

$$\begin{cases} Max\ D = \sqrt{d_S \times d_A} \\ s.t.\ 10\ \text{m} \le depth \le 20\ \text{m} \\ 45 \le angle \le 60 \\ 300\ \text{m} \le R \le 350\ \text{m} \end{cases} \tag{2}$$

$$d_s = \left(\frac{s(depth, angle, R) - s^L}{s^U - s^L} \right)^{W_1} \tag{3}$$

$$d_a = \left(1 - \frac{a(depth, angle, R) - a^L}{a^U - a^L} \right)^{W_2} \tag{4}$$

where, s^U, s^L and a^U, a^L denote the upper and lower bounds for the displacement response and acceleration response, respectively. W_1 and W_2 are the weighting coefficients around the displacement response and acceleration response, respectively. The multi-objective optimization problem is solved by applying an optimization algorithm to vary the buried depth and curve angle to calculate the optimal configuration of the small-radius curved tunnel through the Design-Expert software. For both objectives, the same importance parameter (r) is set. After many calculations, it is more reasonable that a displacement objective weight of 5 and an acceleration objective weight of 4 were specified within the weight setting range, to achieve an emphasis on the displacement objective. The Design-Expert software can search for one or more points in the factor domain depending on

the objective optimization characteristics to maximize the value of the objective function. Figure 9 shows the relationship between the expectation function and the design variables of buried depth and curve angle. It can be seen that the value of the objective function increases with increasing buried depth: when the buried depth reaches 10–17 m, the expected value increases slowly, and when the buried depth is 17–20 m, the expected value increases sharply. The expected value of the expectation function increases as the angle decreases, but the overall rate of increase is slow.

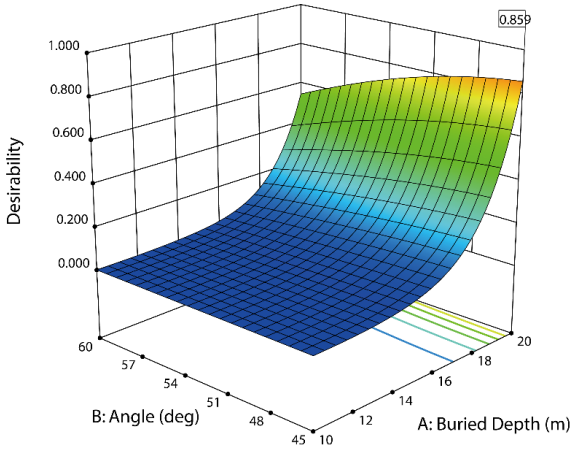

Figure 9. Expectation functions and design variables in relation to surface for point A.

Table 9 gives the geometrical parameters values of point A of the small-radius curved tunnel under seismic excitation and with minimum displacement and acceleration conditions. In Table 9, the geometrical parameters that meet the requirements of the multi-objective optimization are the maximum buried depth, the minimum curve angle and the maximum curve radius within the domain. The expected value of the results is 0.859, which is generally in line with expectations.

Table 9. Design-Expert optimization design results for point A.

Depth (m)	Angle (deg)	*R* (m)	*s* (m)	*a* (m/s^2)	Expected Value
20.000	45.002	350.000	0.114	2.363	0.859

The relationship between the B-point expectation function and the design variables of buried depth and curve angle of curved tunnel is shown in Figure 10. It can be seen from Figure 10 that the expected value of the expectation function increases with increasing buried depth: when the angle is taken as 45–52°, the expected value increases with the increase in buried depth, and the function value of the expectation function decreases slightly when the buried depth is 19 m–20 m. When the angle is taken as 52–60°, the expectation increases monotonically with increasing buried depth. Once both the buried depth and the angle are taken to their maximum values, the expected value of the expectation function reaches its maximum value, which is 0.725.

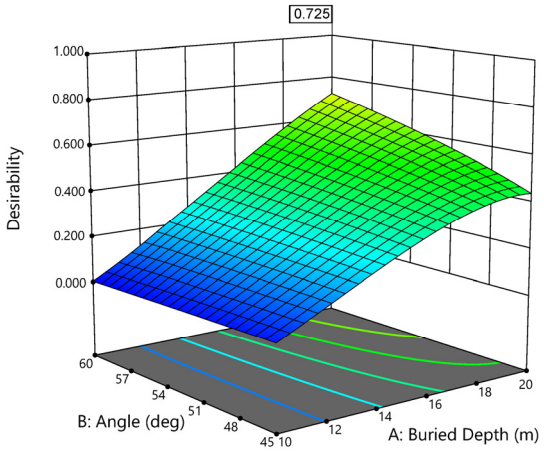

Figure 10. Expectation function and design variable relation surface for point B.

Table 10 gives the values of the geometrical parameters for the small-radius curved tunnel under seismic excitation and with conditions of minimum displacement and acceleration. As can be seen from the table, the geometrical parameters that meet the requirements of the multi-objective optimization are the maximum buried depth, the maximum curve angle and the maximum curve radius within the domain, with an expected value of 0.725 as a result.

Table 10. Design expert optimized design results for point B.

Depth (m)	Angle (deg)	*R* (m)	*S* (m)	*a* (m/s^2)	Expected Value
20.000	60.000	349.999	0.113	8.315	0.725

Comparing the results of the optimization at point A, the optimization at point A results in the maximum buried depth, the minimum curve angle and the maximum curve radius within the domain, while the optimization at point B results in the maximum buried depth, the maximum curve angle and the maximum curve radius within the domain, as shown in Table 10. Here, combined with the analysis in Tables 6 and 7, the F-value of the curve angle in the RSM analysis of point B is greater than the F-value of point A, and the *p*-value of the curve angle is smaller than the *p*-value of point A. This means that the RSM analysis at point B has a more significant effect on the MOOD results regarding the curve angles, and the data are also more reliable. Therefore, the multi-objective optimization results for point B are chosen, i.e., the geometrical parameters that meet the requirements of the MOOD are the maximum buried depth, the maximum curve angle and the maximum curve radius within the domain.

To verify the accuracy of the Design-Expert optimization design results, the finite element simulations method (FEM) was carried out based on the geometry obtained from the results. A comparison of the optimized design results with the FEM results is shown in Table 11, where a comparison of the data shows that the error rate of the FEM simulation and RSM optimal solution prediction results regarding the displacement response is 2.63% and that regarding the acceleration response is 1.90%. It can be seen that the results are basically the same and, therefore, the optimization results can be considered valid.

Table 11. Comparison between optimization design results and FEM results.

	s (m)	a (m/s^2)
FEM Results	0.116	8.473
RSM prediction	0.113	8.315
Error	2.63%	1.90%

5. Conclusions

In this paper, the effects of geometric factors such as buried depth, curve angle and curve radius on the seismic response of a small-radius curved tunnel are discussed by using response surface methodology (RSM) through experimental design and finite element simulation calculation. The displacement and acceleration of the small-radius curved tunnel under seismic excitation are modelled as a function of the corresponding geometrical parameters by means of the RSM. Based on this model, a MOD approach is used to study the optimal geometric parameter configuration of the small-radius curved tunnel. The main conclusions thus obtained are as follows.

(1) The buried depth of the small-radius curved tunnel is the most important factor affecting displacement. When the buried depth increases, the displacement response of the small-radius curved tunnel under seismic excitation decreases, while the displacement response of the curved tunnel increases slightly as the angle increases. For point A of the small-radius curved tunnel, the angle of the curved tunnel and the radius of the curve do not offer significant implications for the displacement response. For point B of the small-radius curved tunnel, the effect of curve angle on the displacement response is more significant, while the effect of curve radius on the displacement response is not significant. As the buried depth increases, the displacement response of the small-radius curved tunnel under seismic excitation decreases, while the displacement response of the curved tunnel increases slightly as the angle increases.

(2) The buried depth of the small-radius curved tunnel is the key parameter affecting the acceleration response values. For point A of the small-radius curved tunnel, the radius of the curve has a significant effect on the acceleration response values and the angle of the curve does not offer significant implications for the acceleration response values. The minimum acceleration is obtained when both the buried depth and the radius of the curve are taken to be the minimum values. For point B of the small-radius curved tunnel, the effect of curve angle on the acceleration response value is slightly significant and the implication of curve radius on the acceleration response is not significant. As the buried depth increases, the overall acceleration response of the small-radius curved tunnel under seismic excitation tends to increase, with the minimum value of the acceleration response occurring around the minimum point of the buried depth, and the minimum acceleration is obtained when the buried depth is taken to be the minimum and the curve angle is taken to be the maximum.

(3) The optimum geometric parameter configuration for the small-radius curved tunnel can be obtained by taking the maximum buried depth, the maximum curve angle and the maximum curve radius within the domain.

Author Contributions: Conceptualization, methodology, X.F., Y.X. and F.Y.; software, Y.X., S.L. and F.Y.; validation, Y.X., S.L. and F.Y.; formal analysis, Y.X. and S.L.; investigation, Y.X.; resources, funding acquisition, S.L. All authors have read and agreed to the published version of the manuscript.

Funding: This research was funded by the Natural Science Research of Higher Education Institutions in Jiangsu Province, China (grant number 18KJB560001). Changzhou Leading Innovative Talents Introduction and Cultivation Project (grant number CQ20220100).

Institutional Review Board Statement: Not applicable.

Informed Consent Statement: Not applicable.

Data Availability Statement: The results presented in this study are available on request from the corresponding author. The data are not publicly available due to the reason that the authors are conducing further analysis on the same structural model.

Conflicts of Interest: The authors declare no conflict of interest.

Nomenclature

a	Acceleration response of the curved tunnel
a^L	Denotes the lower bound for the acceleration response
a^U	Denotes the upper bound for the acceleration response
angle	Angle deg for the curved tunnel
depth	Buried depth of the curved tunnel
R	Curve radius for the curved tunnel
s	Displacement response of the curved tunnel
s^L	Denotes the lower bound for the displacement response
s^U	Denotes the upper bound for the displacement response
W_1	The weighting factor for the displacement response
W_2	The weighting factor for the acceleration response
x	A vector of k design variables of structural geometry
x^L	Lower bounds of designed variables of structural geometry
x^U	Upper bounds of designed variables of structural geometry

References

1. Choi, J.S.; Lee, J.S.; Kim, J.M. Nonlinear Earthquake Response Analysis of 2-D Underground Structures with Soil-structures Interaction Including Separation and Sliding at Interface. In *15th ASCE Engineering Mechanics Conference*; Columbia University: New York, NY, USA, 2002.
2. Chen, J.; Jiang, L.; Li, J.; Shi, X. Numerical simulation of shaking table test on utility tunnel under non-uniform earthquake excitation. *Tunn. Undergr. Space Technol.* **2020**, *30*, 205–216. [CrossRef]
3. Ding, J.H.; Jin, X.L.; Guo, Y.Z.; Li, G.G. Numerical simulation for large-scale seismic response analysis of immersed tunnel. *Eng. Struct.* **2006**, *28*, 1367–1377. [CrossRef]
4. Kontoe, S.; Zdravkovic, L.; Potts, D.M.; Menkiti, C.O. Case study on seismic tunnel response. *Can. Geotech. J.* **2008**, *45*, 1743–1764. [CrossRef]
5. Shukla, D.K.; Rizzo, P.C.; Stephenson, D.E. Earthquake load analysis of tunnels and shafts. In *21st US Symposium on Rock Mechanics (USRMS)*; OnePetro: Richardson, TX, USA, 1980.
6. Anastasopoulos, I.; Gerolymos, N.; Drosos, V.; Georgarakos, T.; Kourkoulis, R.; Gazetas, G. Behavior of deep immersed tunnel under combined normal fault rupture deformation and subsequent seismic shaking. *Bull. Earthq. Eng.* **2008**, *6*, 213–239. [CrossRef]
7. Sánchez-Merino, A.L.; Fernández-Sáez, J.; Navarro, C. Simplified longitudinal seismic response of tunnels linings subjected to surface waves. *Soil Dyn. Earthq. Eng.* **2009**, *29*, 579–582. [CrossRef]
8. Dowding, C.H.; Rozan, A. Damage to rock tunnels from earthquake shaking. *J. Geotech. Eng. Div.* **1978**, *104*, 175–191. [CrossRef]
9. Mu, J.H.; Wang, G.B. Analysis of seismic response of small-radius planar curved tunnel. *J. Geotech. Eng.* **2019**, *41* (Suppl. S2), 197–200. (In Chinese)
10. Liu, J.B.; Du, Y.; Du, X.; Wang, Z.; Wu, J. 3D viscous-spring artificial boundary in time domain. *Earthq. Eng. Eng. Vib.* **2006**, *5*, 93–102. [CrossRef]
11. Liu, J.B.; Lv, Y.D. A direct method for analysis of dynamic soil-structure interaction based on interface idea. *Dev. Geotech. Eng.* **1998**, *83*, 261–276. [CrossRef]
12. Du, X.L.; Zhao, M. Analysis method for seismic response of arch dams in time domain based on viscous-spring artificial boundary condition. *J. Hydraul. Eng.* **2006**, *37*, 1063–1069. (In Chinese)
13. Qiu, D.P.; Chen, J.Y.; Xu, Q. 3-D numerical analysis on seismic responses of the underground large scale frame structure under near-fault ground motions. *Tunn. Undergr. Space Technol.* **2019**, *91*, 103020. [CrossRef]
14. Li, Y.; Wang, G.; Wang, Y. Parametric investigation on the effect of sloping topography on horizontal and vertical ground motions. *Soil Dyn. Earthq. Eng.* **2022**, *159*, 107346. [CrossRef]
15. Sun, Q.; Dias, D.; e Sousa, L.R. Soft soil layer-tunnel interaction under seismic loading. *Tunn. Undergr. Space Technol.* **2020**, *98*, 103329. [CrossRef]
16. Myers, R.H.; Khuri, A.I.; Carter, W.H. Response surface methodology: 1966–l988. *Technometrics* **1989**, *31*, 137–157. [CrossRef]
17. Box, G.E.; Wilson, K.B. On the experimental attainment of optimum conditions. In *Breakthroughs in Statistics*; Springer: New York, NY, USA, 1992; pp. 270–310. [CrossRef]
18. Box, G.E.; Draper, N.R. A basis for the selection of a response surface design. *J. Am. Stat. Assoc.* **1959**, *54*, 622–654. [CrossRef]
19. Hill, W.J.; Hunter, W.G. A review of response surface methodology: A literature survey. *Technometrics* **1996**, *8*, 571–590. [CrossRef]
20. Mead, R.; Pike, D.J. A review of response surface methodology from a biometric viewpoint. *Biometrics* **1975**, *31*, 803–851. [CrossRef]
21. Myers, R.H.; Montgomery, D.C.; Anderson-Cook, C.M. *Response Surface Methodology: Process and Product Optimization Using Designed Experiments*; John Wiley & Sons: Hoboken, NJ, USA, 2016.
22. Hou, S.; Li, Q.; Long, S.; Yang, X.; Li, W. Multiobjective optimization of multi-cell sections for the crashworthiness design. *Int. J. Impact Eng.* **2008**, *35*, 1355–1367. [CrossRef]

23. Baroutaji, A.; Morris, E.; Olabi, A.G. Quasi-static response and multi-objective crashworthiness optimization of oblong tube under lateral loading. *Thin-Walled Struct.* **2014**, *82*, 262–277. [CrossRef]
24. Hou, S.; Li, Q.; Long, S.; Yang, X.; Li, W. Crashworthiness design for foam filled thin-wall structures. *Mater. Des.* **2009**, *30*, 2024–2032. [CrossRef]
25. Salehghaffari, S.; Rais-Rohani, M.; Najafi, A. Analysis and optimization of externally stiffened crush tubes. *Thin-Walled Struct.* **2011**, *49*, 397–408. [CrossRef]